

Article

High Power and Short Pulse Width Operation of Passively Q-Switched Er:Lu₂O₃ Ceramic Laser at 2.7 μm

Li Wang ¹ , Haitao Huang ², Deyuan Shen ^{1,*}, Jian Zhang ² and Dingyuan Tang ²

¹ Department of Optical Science and Engineering, Fudan University, Shanghai 200433, China; wanglilaser@163.com

² Jiangsu Key Laboratory of Advanced Laser Materials and Devices, School of Physics and Electronic Engineering, Jiangsu Normal University, Xuzhou 221116, China; hht840211@163.com (H.H.); jzhang@jsnu.edu.cn (J.Z.); edytang@ntu.edu.sg (D.T.)

* Correspondence: shendy@fudan.edu.cn; Tel.: +86-21-6564-2159

Received: 26 April 2018; Accepted: 16 May 2018; Published: 16 May 2018



Abstract: Using a low non-saturable loss Bragg-reflector-based semiconductor saturable mirror, a passively Q-switched Er:Lu₂O₃ ceramic laser at 2.7 μm demonstrated short pulse-width and efficient operation, generating stable pulses of 70 ns pulse-width and ~71 kHz repetition rates. Over 692 mW of average output power was measured, corresponding to a pulse energy of ~9.8 μJ. In a modified resonator design of reduced round-trip time, pulses of 32 ns duration were generated. The achieved results suggest that Er:Lu₂O₃ ceramic could be a promising gain medium for efficient and high power pulsed laser generation at 2.7 μm. The prospects for further improvement in laser performance at this wavelength are discussed.

Keywords: mid-infrared laser materials; transparent ceramic; passively Q-switched lasers

1. Introduction

Solid-state lasers based on Er³⁺ emitting around 3 μm have attracted significant attention because of their potential for numerous applications, such as laser microsurgery, laser radar, plastic and polymer processing, and pumps for longer wavelength oscillations [1–3]. Lasing on the ⁴I_{11/2} → ⁴I_{13/2} transition of Er³⁺ ions has been widely studied with a variety of host materials at the mentioned spectral region [4–10]. Conventionally, the lifetime of the upper level is lower than the terminated one. For preventing the self-terminating effect of the mentioned transition, high Er³⁺-ion doping concentration is typically required to depopulate the lower laser level by using the concentration dependent energy transfer up-conversion process. In view of the large quantum defect with the most spread ⁴I_{15/2} → ⁴I_{11/2} → ⁴I_{13/2} pump-lase scheme (~70%) and the shallow pump absorption result from the high doping level, a large amount of heat would concentrate near the surface of the gain media. The induced temperature gradient may lead to distortion of the laser mode and strong thermal lensing with pronounced spherical aberrations. In this regard, thermally advanced host materials, such as sesquioxides, are of great interest for high power Er 3-μm laser operations [9,10].

Lu₂O₃ is an appealing sesquioxide, which exhibits low phonon energy (618 cm⁻¹) and a wide spectral transparency range (0.225–8 μm), which favors its applications as a mid-infrared laser gain medium [11]. In addition, its thermal conductivity stays high even at a high Er³⁺-ion doping level, because of the similar atomic mass of the Lu³⁺ and Er³⁺ ions [9]. Recently, Er:Lu₂O₃ crystal was proven to be an excellent sesquioxide for power scaling, and efficient laser operation at 2.84 μm has been demonstrated [9]. Due to the difficulty in growing high quality and large-volume sesquioxide crystals, which originates from their high melting point (>2400 °C), intense research efforts have been

focused on the development of sesquioxide ceramic lasers [10–16]. Polycrystalline Er:Lu₂O₃ ceramic has recently been fabricated successfully and spectroscopically characterized [13,14]. In 2014, the first continuous-wave (CW) laser radiation of Er:Lu₂O₃ ceramic around 3 μm was reported [15], and very recently, efficient diode pumped CW operation was realized [16].

Q-switched mid-infrared (MIR) lasers capable of producing nanosecond pulses with a high peak power are of great interest for applications as a pump source of longer wavelength oscillations, and for using in laser microsurgery and materials processing. Passively Q-switched approaches offer advantages over the active ones in terms of simplicity, compactness and they have no need of extra electric devices. A variety of saturable absorbers (SAs), such as graphene, black phosphorus (BP), MoS₂, ReS₂, graphitic carbon nitride (g-C₃N₄), Bi₂Te₃, have so far been used for Q-switching of ~3-μm lasers [17–23]. Up to watt-level outputs at 2.84 μm have been demonstrated using Er:Lu₂O₃ crystal, generating pulses of ~350 ns durations and ~100 kHz repetition rates [21–23]. Compared with the newly developed two-dimensional (2D) materials-based SAs, the semiconductor saturable absorber mirror (SESAM) has many advantages since the key parameters, e.g., the absorption recovery time and the modulation depth, can be tailored in a wide range [24]. Recently, the successful Q-switched and mode-locked operation of Er:ZBLAN fiber lasers has been demonstrated [25,26]. In these systems, specifically structured metal-reflector-based SESAMs were utilized. For this type of SESAMs, the InAs absorber layer was sandwiched between an Au-coated mirror and a GaAs wafer. In general, metal-reflector-based SESAMs have a relatively high non-saturable loss of >5% induced by the included buffer layer, substrate and Au bottom mirror, and hence may limit the performance of 3-μm solid-state lasers [27,28]. Q-switched operation of Er:Lu₂O₃ ceramic laser using metal-reflector-based absorber has very recently been demonstrated, generating 60 mW of average output power with 660 ns of pulse duration [29].

In this paper, we report on the demonstration of passively Q-switched operation of 2.7-μm Er:Lu₂O₃ ceramic laser with improved performance using a Bragg-reflector-based SESAM of modified band-gap and reduced non-saturated loss. With a thermal-stable resonator design, stable pulse trains of 70 ns pulse width and ~71 kHz repetition rate were generated. An average output power of 692 mW was measured, corresponding to a pulse energy of 9.8 μJ and a peak power of 0.14 kW. Using a modified resonator design of reduced round-trip time, pulses of 32 ns duration were generated. Results presented in this paper suggest that Er:Lu₂O₃ ceramic could be a promising gain medium for high power and efficient nanosecond pulse generation in a 2.7-μm wavelength regime.

2. Experimental Details

Figure 1 shows the experimental setup for the passively Q-switched (PSQ) Er:Lu₂O₃ ceramic laser. A compact three mirror, V-shaped cavity design was employed. The resonator comprised a plane pump coupling mirror (M1) with 6.5% transmission at lasing wavelength and high transmission (>90%) at the pump wavelength, a concave dichroic mirror (M2, 50 mm radius of curvature) and a reflection-type SESAM. The concave dichroic mirror was high-reflection coated at the lasing wavelength and anti-reflection coated at the pump wavelength, which was used to filter out the residual pump light and minimize its influence on the SA. The laser output was extracted and separated from the pump light by a dichroic mirror (M3).

The gain medium was an uncoated 10.6-mm-long, 7 at. % Er:Lu₂O₃ ceramic, which was wrapped with indium foil and mounted on a water-cooled heat-sink for heat removal. The physical length of the laser resonator was around 55 mm, and the spacing between M1 and M2 was ~35 mm. Based on the ABCD matrix analysis, the calculated stable zone for the thermal focal length was in the range of from ~120 mm to ~5 mm. The pump source used in the experiment was a fiber coupled laser diode, and its center wavelength was locked at 976 nm with a bandwidth less than 0.3 nm. The delivery fiber has a core diameter of 105 μm and a numerical aperture (NA) of 0.22. The pump light was launched into the gain medium through a telescopic lens system, and the spot diameter was around 360 μm. Under an absorbed pump power of ~10 W, the thermal focal length in the Er:Lu₂O₃ ceramic was

measured to be around 50 mm according to resonator transform circle theory. In the range of 120 mm to 50 mm thermal focal length, the calculated radius of the laser mode in the gain medium varied from $\sim 250 \mu\text{m}$ to $\sim 132 \mu\text{m}$.

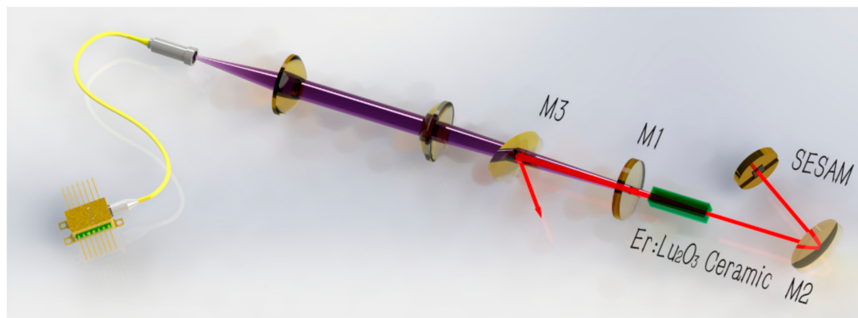


Figure 1. Experimental setup for the passively Q-switched Er:Lu₂O₃ ceramic laser.

The passive Q-switch used in the experiment was a piece of commercial SESAM, which was designed to operate in the wavelength range of 2700–2900 nm (BATOP, model SAM-2800-3-12.7g). The SESAMs have a modulation depth of $\sim 2\%$, a non-saturable loss of $\sim 1\%$, and a relaxation time constant of ~ 10 ps. To measure the laser output power, a thermopile power meter (OPHIR 30A-BB-18) was used in the experiment. The output spectra of the laser output were analyzed using a Fourier Transform Infrared Spectroscopy system (Thorlabs OSA205C) whose resolution was ~ 0.2 nm around $\sim 3 \mu\text{m}$.

3. Experimental Results and Discussion

With a HR mirror replacing the SESAM, CW lasing characteristics of the Er:Lu₂O₃ ceramic were evaluated at first. The output power as a function of the absorbed pump power is shown in Figure 2. The ceramic laser reached threshold at an absorbed pump power of 1.7 W. Under an absorbed pump power of 9.4 W, a maximum output power of 0.95 W was obtained, corresponding to a slope efficiency with respect to the absorbed pump power of 12.9%. Then we used the SESAM as the SA and cavity end mirror. The average output power of the Er:Lu₂O₃ ceramic laser in Q-switched mode of operation is presented in Figure 2. It can be seen that the threshold was increased to 2.3 W and the average output power increased almost linearly with respect to the absorbed pump power up to the maximum pump power of 9.4 W. Under the absorbed pump power of 9.4 W, the laser produced an output power of 0.69 W at 2716 nm with a spectrum bandwidth of ~ 0.2 nm, as shown in the inset of Figure 2, corresponding to a slope efficiency of $\sim 9.7\%$. The decreased slope efficiency compared to the CW operation can be attributed to the intrinsic non-saturable losses of the SA.

With an infrared detector (PVI-10.6, ~ 1.5 ns response time) monitoring the laser temporal behavior, the real-time laser output pulses were recorded by a digital oscilloscope (Keysight DSO104A, bandwidth: 1 GHz). The measured pulse duration and the pulse repetition rate as a function of the absorbed pump power are presented in Figure 3. The pulse duration was 81 ns near the threshold and shows a slight decrease with an increase in the absorbed pump power, while the repetition rate monotonically increased from 3.1 kHz to 71 kHz as the absorbed pump power varied from 2.3 W to 9.4 W. At an absorbed pump power of 9.4 W, the minimum pulse width of 70 ns was obtained, which is nearly an order of magnitude narrower than previously reported for the PSQ Er:Lu₂O₃ ceramic laser [29]. Given that the PSQ laser properties related to the SA, the improved performance in the present work can be attributed to the following reasons: low non-saturable loss of the Bragg-reflector-based SESAM itself results in a higher laser gain, while matching the semiconductor band-gap energy with the lasing photon energy further decreases the saturation fluence and the saturation carrier density of the SA, and thus, bleaching the SA is achievable with fewer laser photons, which in turn results in a decreased intracavity loss and an increased laser net gain [30,31].

These cascading effects in the PSQ Er:Lu₂O₃ ceramic laser result in a dramatic increase in output power and lasing efficiency, and a shorter Q-switched laser pulse width [32].

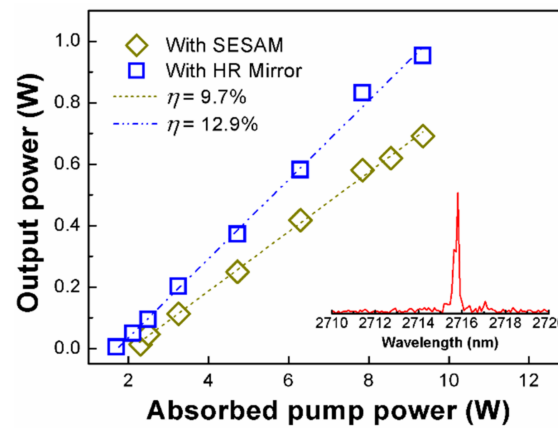


Figure 2. Output power as a function of the absorbed pump power of the Er:Lu₂O₃ ceramic laser under CW and passively Q-switched mode of operation. Inset: laser output spectrum at 2716 nm.

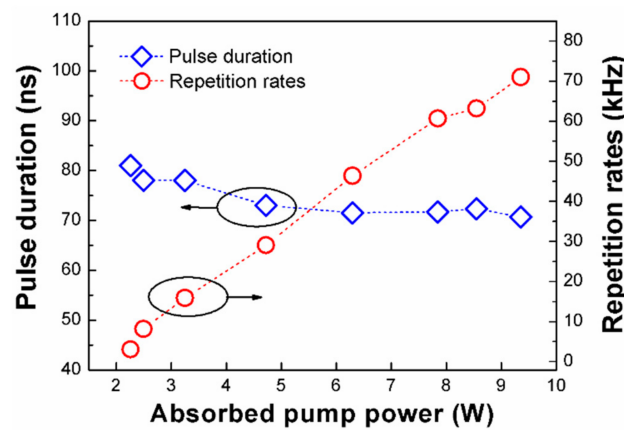


Figure 3. Measured pulse duration and repetition rate as function of the absorbed pump power.

Figure 4 shows the pulse energy and the corresponding pulse peak power as a function of the absorbed pump power. The pulse energy and the peak power show a monotonic increase with respect to the absorbed pump power. Since the absorber is fully saturated, the pulse energy and peak power do not depend noticeably of the pump power. Under an absorbed pump power of 9.4 W, the pulse energy was found to be ~9.8 μ J and corresponds to a peak power of 0.14 kW. To the best of our knowledge, this is the highest peak power reported for the Q-switched Er:Lu₂O₃ laser [23]. The typical pulse profile and the corresponding pulse train for the maximum output power is shown in Figure 5. Pulse to pulse amplitude fluctuation was estimated to be less than 5%.

As a comparison, Table 1 summarizes the results ever produced from the PSQ Er:Lu₂O₃ lasers. The Er:Lu₂O₃ ceramic laser in present work provides similar pulse energy and average output power to the crystal laser, but higher pulse peak power and five times decrease in pulse duration [21–23,29]. Compared to the earlier reported PSQ Er:Lu₂O₃ ceramic laser at 2.7 μ m, the average output power and slope efficiency in the present work have increased by nearly an order of magnitude [29]. This can be attributed to the modified cavity structure with increased utilization efficiency for the pump power, together with the optimized SA parameters with a decreased intracavity insertion loss. It is worth noting, that the pulse duration of 70 ns is close to the limit set by the cavity length and by the SA’s modulation depth [24,33]. Further shortening in pulse duration should be possible by reducing the

cavity length and hence the cavity roundtrip time, for example microchip laser, or/and using a SA with a higher modulation depth.

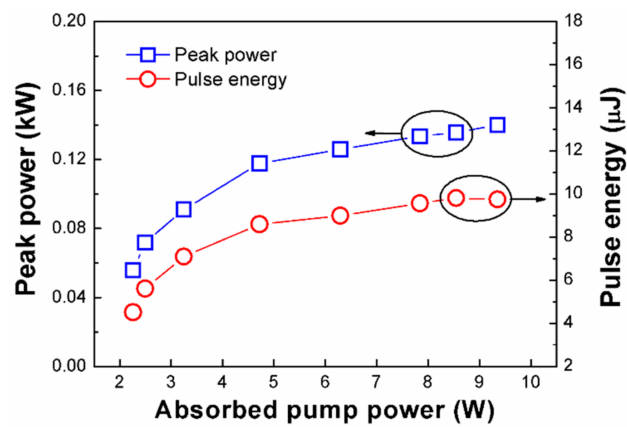


Figure 4. Pulse energy and the corresponding peak power of the Q-switched laser versus the absorbed pump power.

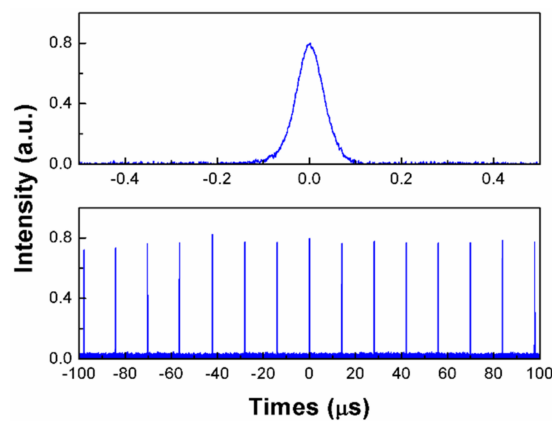


Figure 5. Temporal profiles of the Q-switched pulse trains at different time scales.

Table 1. Comparison of output characteristics of the Er:Lu₂O₃ lasers operating around 3 μm passively Q-switched by various SAs reported so far.

Gain Medium	SA	Wavelength, μm	Pulse Width, ns	Output Power, mW	Pulse Energy, W	Peak Power, W	Ref.
Er:Lu ₂ O ₃ crystal	BP	2.84	359	755	7.1	19.2	[21]
	MoS ₂	2.84	335	1030	8.5	23.8	[22]
	g-C ₃ N ₄	2.84	351	1090	11.1	31.6	[23]
Er:Lu ₂ O ₃ ceramic	SESAM	2.716	660	60	1.8	2.7	[29]
	SESAM	2.716	70	692	9.8	139.2	This work

As a proof-of-principle experiment, the lasing characteristics of the PSQ Er:Lu₂O₃ ceramic were further evaluated with a simple, low-loss, two-mirror cavity. In this configuration we placed the SESAM slightly closer to the Er:Lu₂O₃ ceramic so that the physical length of the cavity was reduced to 19 mm. When the absorbed pump increased to greater than 2.1 W, Q-switched pulses of ~40-ns were produced. With the increase in the pump power, pulses of 32-ns duration were obtained. Note that the pulse duration of 32 ns is close to the limit set by the cavity length as well [24]. This implies that constructing an efficient microchip-type Q-switched Er:Lu₂O₃ ceramic laser and generating sub-nanosecond pulses with MHz repetition rates should be possible [24,25]. Due to the influence of

the unabsorbed pump on the SA, the PSQ laser operation was not as stable as the first configuration [34]. Further optimization should be provided by eliminating the residual pump via placing a dichroic filter after the laser element or applying dichroic coatings on the output face of the laser gain medium.

4. Conclusions

Efficient passive Q-switching of a Er:Lu₂O₃ ceramic laser with Bragg-reflector-based SESAM has been demonstrated. Under an absorbed pump power of 9.4 W, stable Q-switched laser pulses of 70 ns in duration, 0.14 kW in peak power and 9.8 μJ in energy were obtained. Control of the pulse duration by using a cavity length of 19 mm was studied as well, and laser pulses of 32 ns in duration, close to the limit set by the cavity length, were obtained. To our knowledge, this is the shortest pulse duration and highest peak power ever produced from a Q-switched Er:Lu₂O₃ laser. This paper reveals that the Er:Lu₂O₃ ceramic is a promising laser gain medium in achieving efficient and high power 2.7-μm nanosecond pulses.

Author Contributions: D.S., L.W. and D.T. conceived and designed the experiments; L.W., J.Z. and H.H. performed the experiments, analyzed the data and wrote the paper.

Acknowledgments: This work is supported by the National Natural Science Foundation of China (Grant No. U1730119 and 61505072), and the Priority Academic Program Development of Jiangsu Higher Education Institutions (PAPD).

Conflicts of Interest: The authors declare no conflict of interest.

References

- Jackson, S.D. Towards high-power mid-infrared emission from a fibre laser. *Nat. Photonics* **2012**, *6*, 423–431. [[CrossRef](#)]
- Bubb, D.M.; Haglund, R.F. *Pulsed Laser Deposition of Thin Films: Applications-Led Growth of Functional Materials*, 1st ed.; John Wiley & Sons: New York, NY, USA, 2006; pp. 41–59. ISBN 9780470052129.
- Hudson, D.D.; Antipov, S.; Li, L.; Alamgir, I.; Hu, T.; Amraoui, M.E.; Messaddeq, Y.; Rochette, M.; Jackson, S.D.; Fuerbach, A. Toward all-fiber supercontinuum spanning the mid-infrared. *Optica* **2017**, *4*, 1163–1166. [[CrossRef](#)]
- Jensen, T.; Diening, A.; Huber, G.; Chai, B.H. Investigation of diode-pumped 2.8-μm Er:LiYF₄ lasers with various doping levels. *Opt. Lett.* **1996**, *21*, 585–587. [[CrossRef](#)] [[PubMed](#)]
- Zioleck, C.; Ernst, H.; Will, G.F.; Lubatschowski, H.; Welling, H.; Ertmer, W. High-repetition-rate, high-average-power, diode-pumped 2.94-μm Er:YAG laser. *Opt. Lett.* **2001**, *26*, 599–601. [[CrossRef](#)]
- Chen, J.; Sun, D.; Luo, J.; Zhang, H.; Dou, R.; Xiao, J.; Zhang, Q.; Yin, S. Spectroscopic properties and diode end-pumped 2.79 μm laser performance of Er,Pr:GYSGG crystal. *Opt. Express* **2013**, *21*, 23425–23432. [[CrossRef](#)] [[PubMed](#)]
- Shen, B.J.; Kang, H.X.; Sun, D.L.; Zhang, Q.L.; Yin, S.T.; Chen, P.; Liang, J. Investigation of laser-diode end-pumped Er: YSGG/YSGG composite crystal lasers at 2.79 μm. *Laser Phys. Lett.* **2014**, *11*, 015002. [[CrossRef](#)]
- You, Z.; Wang, Y.; Xu, J.; Zhu, Z.; Li, J.; Wang, H.; Tu, C. Single-longitudinal-mode Er:GGG microchip laser operating at 2.7 μm. *Opt. Lett.* **2015**, *40*, 3846. [[CrossRef](#)] [[PubMed](#)]
- Li, T.; Beil, K.; Kränkel, C.; Huber, G. Efficient high-power continuous wave Er:Lu₂O₃ laser at 2.85 μm. *Opt. Lett.* **2012**, *37*, 2568–2570. [[CrossRef](#)] [[PubMed](#)]
- Sanamyan, T.; Kanskar, M.; Xiao, Y.; Kedlaya, D.; Dubinskii, M. High power diode-pumped 2.7-μm Er³⁺:Y₂O₃ laser with nearly quantum defect-limited efficiency. *Opt. Express* **2011**, *19*, A1082–A1087. [[CrossRef](#)] [[PubMed](#)]
- Krankel, C. Rare-earth-doped sesquioxides for diode-pumped high-power lasers in the 1-, 2-, and 3-μm spectral range. *IEEE J. Sel. Top. Quantum Electron.* **2015**, *21*, 250–262. [[CrossRef](#)]
- Ikesue, A.; Aung, Y.L. Ceramic laser materials. *Nat. Photonics* **2018**, *2*, 721–727. [[CrossRef](#)]
- Qiao, X.; Huang, H.; Yang, H.; Zhang, L.; Wang, L.; Shen, D.; Zhang, J.; Tang, D. Fabrication, optical properties and LD-pumped 2.7 μm laser performance of low Er³⁺ concentration doped Lu₂O₃ transparent ceramics. *J. Alloys Compd.* **2015**, *640*, 51–55. [[CrossRef](#)]

14. Uehara, H.; Yasuhara, R.; Tokita, S.; Kawanaka, J.; Murakami, M.; Shimizu, S. Efficient continuous wave and quasi-continuous wave operation of a 2.8 μm Er:Lu₂O₃ ceramic laser. *Opt. Express* **2017**, *25*, 18677–18684. [[CrossRef](#)] [[PubMed](#)]
15. Wang, L.; Huang, H.; Shen, D.; Zhang, J.; Chen, H.; Wang, Y.; Liu, X.; Tang, D. Room temperature continuous-wave laser performance of LD pumped Er:Lu₂O₃ and Er:Y₂O₃ ceramic at 2.7 μm . *Opt. Express* **2014**, *22*, 19495–19503. [[CrossRef](#)] [[PubMed](#)]
16. Uehara, H.; Tokita, S.; Kawanaka, J.; Konishi, D.; Murakami, M.; Shimizu, S.; Yasuhara, R. Optimization of laser emission at 2.8 μm by Er:Lu₂O₃ ceramics. *Opt. Express* **2018**, *26*, 3497–3507. [[CrossRef](#)] [[PubMed](#)]
17. Zhu, X.; Zhu, G.; Wei, C.; Kotov, L.V.; Wang, J.; Tong, M.; Norwood, R.A.; Peyghambarian, N. Pulsed fluoride fiber lasers at 3 μm . *J. Opt. Soc. Am. B* **2017**, *34*, A15–A28. [[CrossRef](#)]
18. Nie, H.; Zhang, P.; Zhang, B.; Yang, K.; Zhang, L.; Li, T.; Zhang, S.; Xu, J.; Hang, Y.; He, J. Diode-end-pumped Ho,Pr:LiLuF₄ bulk laser at 2.95 μm . *Opt. Lett.* **2017**, *42*, 699–702. [[CrossRef](#)] [[PubMed](#)]
19. You, Z.; Sun, Y.; Sun, D.; Zhu, Z.; Wang, Y.; Li, J.; Tu, C.; Xu, J. High performance of a passively Q-switched mid-infrared laser with Bi₂Te₃/graphene composite SA. *Opt. Lett.* **2017**, *42*, 871–874. [[CrossRef](#)] [[PubMed](#)]
20. Su, X.C.; Nie, H.K.; Wang, Y.R.; Li, G.R.; Yan, B.Z.; Zhang, B.T.; Yang, K.J.; He, J.L. Few-layered ReS₂ as saturable absorber for 2.8 μm solid state laser. *Opt. Lett.* **2017**, *42*, 3502–3505. [[CrossRef](#)] [[PubMed](#)]
21. Fan, M.; Li, T.; Zhao, S.Z.; Li, G.; Gao, X.; Yang, K.; Li, D.; Kränkel, C. Multilayer black phosphorus as saturable absorber for an Er:Lu₂O₃ laser at \sim 3 μm . *Photonics Res.* **2016**, *4*, 181–186. [[CrossRef](#)]
22. Fan, M.; Li, T.; Zhao, S.; Li, G.; Ma, H.; Gao, X.; Kränkel, C.; Huber, G. Watt-level passively Q-switched Er:Lu₂O₃ laser at 2.84 μm using MoS₂. *Opt. Lett.* **2016**, *41*, 540–543. [[CrossRef](#)] [[PubMed](#)]
23. Fan, M.; Li, T.; Li, G.; Ma, H.; Zhao, S.; Yang, K.; Kränkel, C. Graphitic C₃N₄ as a new saturable absorber for the mid-infrared spectral range. *Opt. Lett.* **2017**, *42*, 286–289. [[CrossRef](#)] [[PubMed](#)]
24. Spühler, G.J.; Paschotta, R.; Fluck, R.; Braun, B.; Moser, M.; Zhang, G.; Gini, E.; Keller, U. Experimentally confirmed design guidelines for passively Q-switched microchip lasers using semiconductor saturable absorbers. *J. Opt. Soc. Am. B* **1999**, *16*, 376–388. [[CrossRef](#)]
25. Shen, Y.; Wang, Y.; Luan, K.; Huang, K.; Tao, M.; Chen, H.; Yi, A.; Feng, G.; Si, J. Watt-level passively Q-switched heavily Er³⁺-doped ZBLAN fiber laser with a semiconductor saturable absorber mirror. *Sci. Rep.* **2016**, *6*, 26659. [[CrossRef](#)] [[PubMed](#)]
26. Tang, P.; Qin, Z.; Liu, J.; Zhao, C.; Xie, G.; Wen, S.; Qian, L. Watt-level passively mode-locked Er³⁺-doped ZBLAN fiber laser at 2.8 μm . *Opt. Lett.* **2015**, *40*, 4855–4858. [[CrossRef](#)] [[PubMed](#)]
27. Fluck, R.; Jung, I.D.; Zhang, G.; Kärtner, F.X.; Keller, U. Broadband saturable absorber for 10-fs pulse generation. *Opt. Lett.* **1996**, *21*, 743–745. [[CrossRef](#)] [[PubMed](#)]
28. SAMTM Data Sheet SAM-2900-9-10PS-x, $\lambda=2900\text{nm}$. Available online: www.batop.de/products/saturable-absorber/saturable-absorber-mirror/data-sheet/saturable-absorber-mirror-3000nm/saturable-absorber-mirror-SAM-2900-9-10ps.pdf (accessed on 25 April 2018).
29. Ren, X.; Shen, D.; Zhang, J.; Tang, D. Passive Q-switching of \sim 2.7 μm Er:Lu₂O₃ ceramic laser with a semiconductor saturable absorber mirror. *Jpn. J. Appl. Phys.* **2018**, *57*, 022701. [[CrossRef](#)]
30. Tsou, Y.; Garmire, E.; Chen, W.; Birnbaum, M.; Asthana, R. Passive Q switching of Nd:YAG lasers by use of bulk semiconductors. *Opt. Lett.* **1993**, *18*, 1514–1516. [[CrossRef](#)] [[PubMed](#)]
31. Hadar, J.; Yang, H.J.; Scheller, M.; Moloney, J.V.; Koch, S.W. Microscopic analysis of saturable absorbers: Semiconductor saturable absorber mirrors versus graphene. *J. Appl. Phys.* **2016**, *119*, 053102. [[CrossRef](#)]
32. Paschotta, R. *Field Guide to Laser Pulse Generation*; SPIE Press: Bellingham, WA, USA, 2008; p. 16, ISBN 9780819472489.
33. Wang, L.; Huang, H.T.; Ren, X.J.; Wang, J.; Shen, D.Y.; Zhao, Y.G.; Zhou, W.; Liu, P.; Tang, D.Y. Nanosecond pulse generation at 2.7 μm from a passively Q-switched Er:Y₂O₃ ceramic laser. *IEEE J. Sel. Top. Quantum Electron.* **2018**, *24*, 1600906. [[CrossRef](#)]
34. Lan, R.; Mateos, X.; Wang, Y.; Serres, J.M.; Loiko, P.; Li, J.; Pan, Y.; Griebner, U.; Petrov, V. Semiconductor saturable absorber Q-switching of a holmium micro-laser. *Opt. Express* **2017**, *25*, 4579–4584. [[CrossRef](#)] [[PubMed](#)]

